

Effects of Microwave Processing on the Properties of Nickel Oxide/Zirconia/Ceria Composites

Lucas Batochi Pinheiro^{1,a}, Antonio Eduardo Martinelli^{2,b}
and Fabio Coral Fonseca^{1,c}

¹Instituto de Pesquisas Energéticas e Nucleares, IPEN, S. Paulo, SP, 05508-000, Brazil

²Universidade Federal do Rio Grande do Norte, UFRN, Natal, RN, 59072-970, Brazil

^alucas.pinheiro@usp.br, ^baemart@uol.com.br, ^cfcfonseca@ipen.br

Keywords: Microwave-assisted hydrothermal, coprecipitation, SOFC, impedance spectroscopy.

Abstract. The effect of a microwave-assisted hydrothermal (MWH) treatment on the structural, thermal, and electrical properties of NiO/ZrO₂:8 mol%Y₂O₃(YSZ)/CeO₂ (60/20/20 wt.%) composite was investigated. Powders were synthesized by a hydroxide coprecipitation-impregnation technique, in which Ni and Ce oxides were coprecipitated in a suspension containing YSZ. Simultaneous thermogravimetry and differential thermal analysis revealed that MWH treatment promotes the crystallization of coprecipitated phases. X-ray diffraction analysis was used for phase identification and the calculated lattice parameters indicated the formation of YSZ:CeO₂ solid solution during sintering. Impedance spectroscopy measurements showed that the electrical properties of the composite samples were not significantly affected by the MWH.

Introduction

Ni/ZrO₂:8 mol%Y₂O₃ (YSZ) cermet is the standard solid oxide fuel cells (SOFC) anode. Despite limitations due to low redox stability and sintering of Ni particles at high operating temperatures, this cermet exhibits excellent performance with high electronic conductivity and electrocatalytic activity. Irrespectively of the intense research, such properties of the Ni-cermet are unheard by any other alternative anode reported [1]. Ni content strongly influences the electronic conductivity, requiring volume fractions above the percolation threshold, usually ≥ 30 vol.% [1]. This value can be influenced by many factors, such as porosity, pore size, particle size distribution, and phase contiguity [2], which generally results in lower percolation thresholds [3].

Aiming at high-performance SOFC anodes, chemical synthesis routes are preferred over solid-state reaction mechanism. The chemical routes usually results in final products with higher purity, higher chemical homogeneity, and reduced particle size [4]. The liquid mixture technique [5], combustion [6], sol-gel [7], and coprecipitation [8] are some examples of chemical methods previously reported for the synthesis of Ni/YSZ. It is known that microwave energy can improve reaction kinetics, selectivity, and yield of chemical reactions [9, 10]. Therefore, chemical synthesis methods can benefit from microwave heat treatments. Microwave-heated materials exhibit thermal effects unseen in the conventional convective heating [11]. One of the main effects is the inversion in the temperature gradient, causing an inside out heating due the inverted heat-transfer direction in the irradiated material [11]. As a result, elevated heating rates are attained, whereas heat is generated locally (in the material itself), the heating is more homogeneous and volumetric [12].

In the present study, NiO/YSZ/CeO₂ (60/20/20 wt.%) was synthesized by a mixed hydroxide coprecipitation-impregnation technique followed by a microwave-assisted hydrothermal (MWH) treatment for preparing homogeneous and small-sized Ni particles. The effects of the MWH treatment were investigated on the general properties of the resulting composite.

Experimental

The appropriate amounts of Ni(CH₃COO)₂·4H₂O and Ce(NO₃)₃·6H₂O (Aldrich, $\geq 99\%$) were dissolved in distilled water ($[Ni^{2+}] = 0.1 \text{ mol L}^{-1}$) under continuous magnetic stirring to obtain a homogeneous solution and then heated at 95 °C. The solution containing Ni and Ce salts was added

slowly into a suspension formed by YSZ powder (Tosoh, $\geq 99\%$) dispersed in a $\text{NH}_4\text{OH}:\text{H}_2\text{O}$ precipitant solution (1:1 v/v), kept under constant magnetic stirring. The pH of the resulting suspension containing the precipitated material was adjusted to 9.5. The product was then filtered and washed with distilled water and ethanol several times for complete removal of unwanted ions (NH_4^+ , NO_4^- and $\text{CH}_3\text{COO}^{2-}$). After washing step the material was dried at $100\text{ }^\circ\text{C}$ for 12 h and homogenized in agate mortar. The MWH treatment was performed by placing the as-prepared powder in water suspension into a Teflon container, inserted into an autoclave and heated in microwave oven (800 W, 2.45 GHz) at $130\text{ }^\circ\text{C}$ for 2 h with $10\text{ }^\circ\text{C min}^{-1}$ heating rate. The average pressure achieved in this heating condition was 1.4 atm. Calcining was carried out at $500\text{ }^\circ\text{C}$ for 4 h in air. Uniaxially pressed cylindrical pellets (10 mm diameter) were sintered at $1200\text{ }^\circ\text{C}$ for 3 h.

Thermal decomposition of the as-prepared and MWH treated powders were studied by simultaneous thermogravimetry and differential thermal analysis (TG/DTA, Setaram Labsys). The chemical composition of calcined samples was determined by energy dispersive X-ray fluorescence spectroscopy (EDX, Shimadzu EDX-720). Phase identification was performed by X-ray diffraction (XRD), using $\text{Cu}_{K\alpha 1}$ radiation in a Rigaku Miniflex II. The linear retraction during sintering of green ceramic compacts was monitored from room temperature up to $1400\text{ }^\circ\text{C}$ with $10\text{ }^\circ\text{C min}^{-1}$ heating rate (Setaram Labsys). The electrical properties of pellets sintered at $1200\text{ }^\circ\text{C}$ for 3 h were studied by impedance spectroscopy (IS) in the 1 Hz - 30 MHz frequency range and $100\text{ }^\circ\text{C}$ - $700\text{ }^\circ\text{C}$ temperature range with 200 mV ac amplitude using a Solartron 1260. For IS measurements, silver contacts were deposited onto the parallel surfaces of the samples and cured at $600\text{ }^\circ\text{C}$ for 1 h. The impedance diagrams were normalized with the geometric factor of each pellet. The morphology of polished and thermally attacked surfaces of sintered samples was investigated by scanning electron microscopy with field emission (FEG-SEM) using a FEI Inspect F50 microscope operating at 5 kV.

Results and Discussion

Fig. 1 shows the TG/DTA curves for the as-prepared and MWH samples. The TG profiles (Fig. 1a) are similar for both samples. The initial weight loss ($\sim 3\%$) was observed between room temperature and $\sim 200\text{ }^\circ\text{C}$ and attributed to water release. The sharp weight loss of $\sim 10\%$ between $\sim 200\text{ }^\circ\text{C}$ and $400\text{ }^\circ\text{C}$ is due to nickel hydroxide dehydroxylation, according to the reaction: $\text{Ni}(\text{OH})_2 \rightarrow \text{NiO} + \text{H}_2\text{O}$ [13]. This thermal decomposition implies a weight loss of $\sim 12.5\%$ based on the nominal NiO content (60 wt.%). The small deviation observed in the experimental result ($\sim 10\%$) indicates loss of nickel hydroxide during precipitation by formation of soluble nickel-complexes [14]. The exact experimental weight loss is difficult to determine because there is an additional process in this temperature range. The weight loss of hydrated ceria was observed to occur in the $200\text{--}400\text{ }^\circ\text{C}$ range [15]. During precipitation, Ce^{3+} in solution oxidizes to Ce^{4+} for $\text{pH} > 4.4$: $\text{Ce}^{3+} + \text{H}_2\text{O} \leftrightarrow \text{Ce}(\text{OH})^{3+} + \text{H}^+ + \text{e}^-$ [16]. The complex $\text{Ce}(\text{OH})^{3+}$ hydrolyses to $\text{Ce}(\text{OH})_4$ that can be written as $\text{CeO}_2 \cdot 2\text{H}_2\text{O}$, which dehydrates progressively, i.e., $\text{CeO}_2 \cdot n\text{H}_2\text{O}$ ($n \leq 2$) [15]. Nickel hydroxide has two polymorphs denoted as $\alpha\text{-Ni}(\text{OH})_2$ and $\beta\text{-Ni}(\text{OH})_2$, both with hexagonal structure. The α form consists in a stack of $\text{Ni}(\text{OH})_{2-x}$ positive charged layers, anions (like carbonates and nitrates) and intercalated water molecules [17]. The β form has a brucite-like structure ($\text{Mg}(\text{OH})_2$) without intercalated species [17]. During the precipitation in the presence of NH_4OH solution, the $\beta\text{-Ni}(\text{OH})_2$ polymorph is formed [18]. The exothermic peaks at $\sim 260\text{ }^\circ\text{C}$ and $280\text{ }^\circ\text{C}$ (Fig. 1b) are attributed to ceria [15] and $\beta\text{-Ni}(\text{OH})_2$ crystallization, respectively. Such attributions were confirmed by performing separated thermal analyses of both Ni and Ce coprecipitated precursors (not shown). It is interesting to note that exothermic peaks are suppressed in the MWH sample, suggesting that the MWH treatment promoted the crystallization of the precipitated phases ($\beta\text{-Ni}(\text{OH})_2$ and ceria). The endothermic peak at $\sim 306\text{ }^\circ\text{C}$ associated with the sharp weight loss region is related to the dehydroxylation reaction and was similar to both samples.

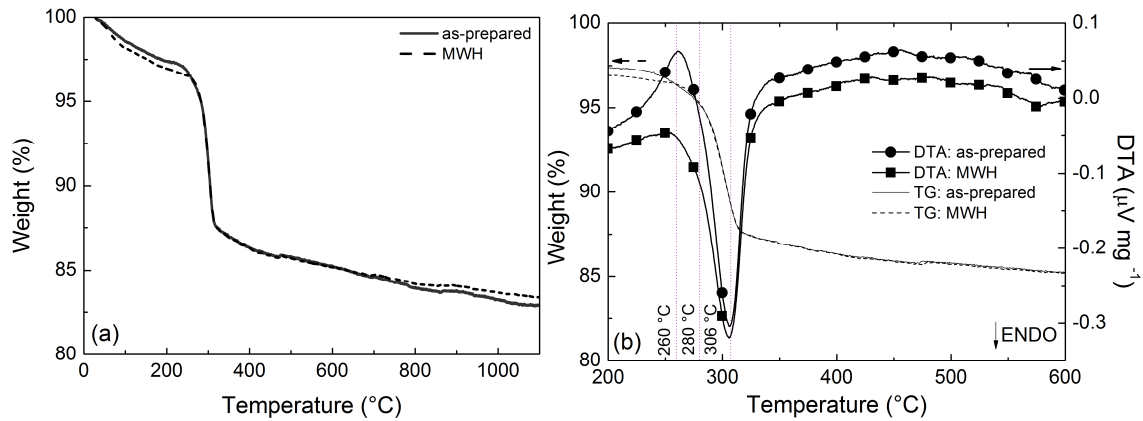


Figure 1 - Thermogravimetric (a) and differential thermal analysis (b) curves for the as-prepared and MWH samples.

Fig. 2 shows the XRD patterns for the as-prepared and MWH powders, before and after calcining at 500°C. The XRD data were indexed according to JCPDS standard files as hexagonal β -Ni(OH)₂ (#14-117), cubic YSZ (#82-1246), cubic CeO₂ (#34-394), and cubic NiO (#47-1049). Although the DTA curves suggested an enhanced crystallization during MWH treatment, no significant difference can be observed in the XRD patterns (Fig. 2a). After calcining (Fig. 2b) the β -Ni(OH)₂ was converted to NiO in accordance with TG/DTA data. The crystallite sizes of the calcined powders were calculated by Scherrer equation with the reflection with the highest relative intensity of each phase. The obtained values were similar for both samples: ~9 nm for NiO, 16 nm for YSZ, and 5 nm for CeO₂. The calculated lattice parameters were similar to those presented in the JCPDS files used for indexing: ~4.18 Å for NiO, ~5.14 Å for YSZ, and ~5.42 Å for CeO₂.

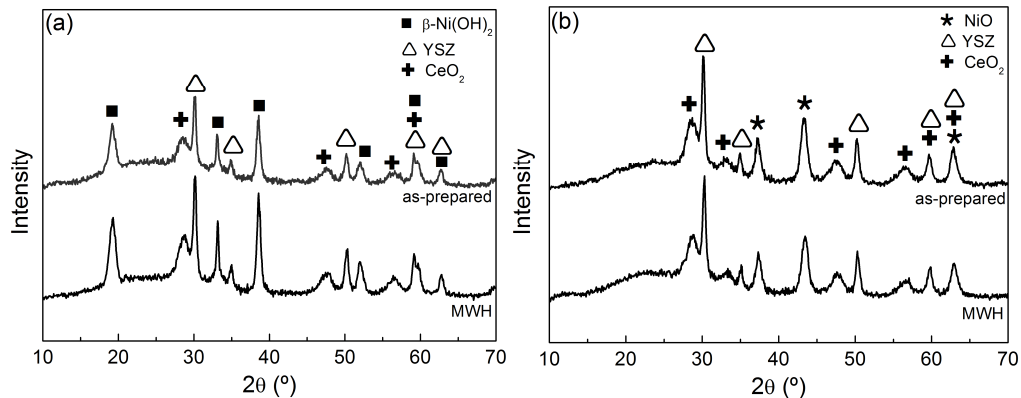


Figure 2 - X-ray diffraction patterns for the as-prepared and MWH powders before (a) and after calcining (b) at 500 °C for 4 h.

A semi-quantitative EDX chemical analysis was carried out in the calcined powders. Table 1 summarizes the results. The measured phase fractions were close to the nominal composition (NiO/YSZ/CeO₂ : 60/20/20 wt.%) with small deviations due to presence of impurities (HfO₂ and SiO₂, arising from the commercial YSZ) and possibly to some loss of nickel during precipitation, as previously discussed.

Table 1 - Oxide phase fractions (wt.%) calculated from EDX data.

Sample	NiO	YSZ	CeO ₂	HfO ₂	SiO ₂
as-prepared	57.9	22.5	18.0	0.9	0.7
MWH	56.8	23.6	18.0	0.8	0.8

The sintering behavior of ceramic compacts was studied by dilatometry analysis, as shown in Fig. 3a. Both samples presented similar linear shrinkage and linear shrinkage rate curves. From room temperature up to ~600 °C a negligible retraction was observed. For T > 600 °C a gradual linear retraction develops. The onset of the sintering process was ~1200 °C and the maximum

densification rate temperature at ~ 1280 °C, as inferred from the derivatives. Sintering process completes at ~ 1350 °C and total linear retractions were 22% and 19% for the as-prepared and MWH samples, respectively. The final apparent density (ρ) and the fraction of the theoretical density ($\% \rho/\rho_T$) were: 6.48 g cm^{-3} (97.1%) and 6.51 g cm^{-3} (98.0%) for the as-prepared sample and the MWH sample, respectively. Fig. 3b shows the XRD of sintered samples. The peaks corresponding to YSZ phase were shifted to lower 2θ values and no peaks of CeO_2 were observed. The calculated lattice parameters for YSZ phase were $\sim 5.25(2)$ Å. Such a lattice parameter is larger than the one calculated for calcined powders, indicating that cerium was incorporated into the YSZ matrix, forming the solid solution $\text{YSZ}:\text{CeO}_2$. The increase in the lattice parameter followed the Vegard law. Given the ceria content with respect to YSZ (35 mol%), the calculated lattice parameters are in good agreement with previously reported data [19].

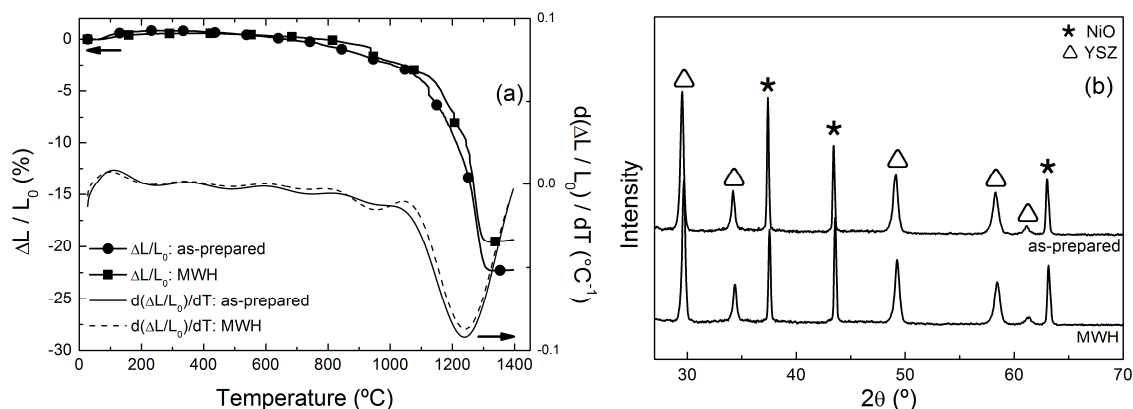


Figure 3 - Linear shrinkage and linear shrinkage rate for ceramic compacts of $\text{NiO}/\text{YSZ}/\text{CeO}_2$ (60/20/20 wt.%) prepared with as-prepared and MWH powders (a). X-ray diffraction patterns for $\text{NiO}/\text{YSZ}/\text{CeO}_2$ samples sintered at 1200 °C for 3 h (b).

Compacts sintered at 1200 °C have apparent densities ρ and ($\% \rho/\rho_T$) of 5.87 g cm^{-3} (90.6%) and 5.81 g cm^{-3} (89.3%) for the as-prepared and MWH samples, respectively. The polished surfaces of sintered samples were studied by FEG-SEM, as shown in Fig. 4. The analyses revealed microstructures with submicrometric grain size with irregular shapes distributed within regions with some porosity and some regions with higher densification. Such regions with different densifications were homogeneously distributed along the observed surfaces. The average grain sizes were roughly estimated: ~ 150 nm for NiO (darker grains) and ~ 350 nm for $\text{YSZ}:\text{CeO}_2$ (brighter grains). However, both samples showed similar features, indicating a weak effect of the MWH treatment on the microstructure of sintered samples.

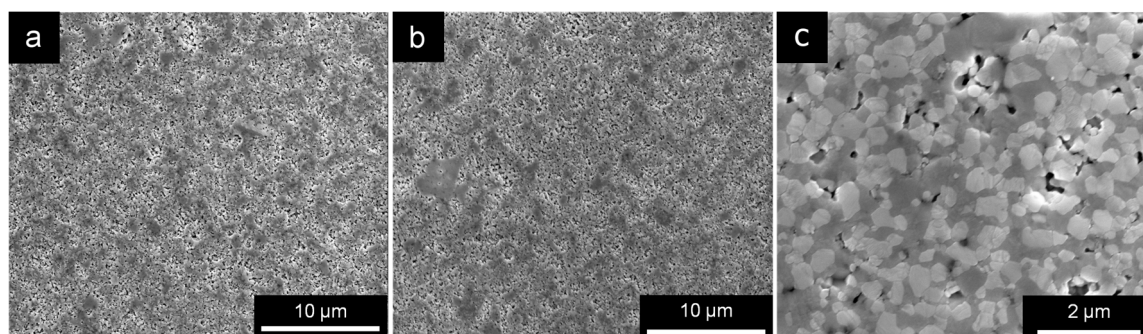


Figure 4 - FEG-SEM images of fractured surfaces of as-prepared (a) and MWH (b, c) sintered compacts.

Impedance diagrams taken at 300 °C and 500 °C for the ceramic compacts, as well as the Arrhenius plots are shown in Fig. 5. The IS diagrams measured at low temperature (≤ 300 °C) exhibit one semicircle with relaxation frequency in the MHz range. The composites exhibit a relatively low electrical resistance due to the high NiO content (~ 60 vol.%), which results in a more pronounced parasitic inductive effect at high frequencies when the measuring temperature is increased. Thus, IS analyzes were limited to the total electrical resistance in the entire temperature

range studied, determined by the low frequency intercept with the real axis. The IS diagrams show a decrease in the electrical resistivity with increasing temperature. However, such a thermally activated behavior is more pronounced in the MWH sample, which assumes lower resistivity values than the as-prepared one for $T > 450$ °C.

The Arrhenius plots (Figs. 5c and 5d) of both samples are similar. The calculated activation energies revealed slightly higher values for the MWH sample, being ~ 0.65 eV for $T < 450$ °C and ~ 0.39 eV for $T > 450$ °C. Such values are lower than the one expected for YSZ (~ 1 eV) and indicate that NiO is the main responsible for the charge transport in the composite. Indeed, the discontinuity in the Arrhenius plots is a characteristic of the NiO transport properties, a feature that evidences the percolation of NiO in the YSZ:CeO₂ matrix [20]. The effect of the MWH on the electrical properties is not very significant, although MWH samples exhibited slightly lower resistivity and higher activation energies. However, it was not possible to correlate such features with microstructural properties of the sintered samples. Detailed FEG-SEM analyses are underway to further investigate this point.

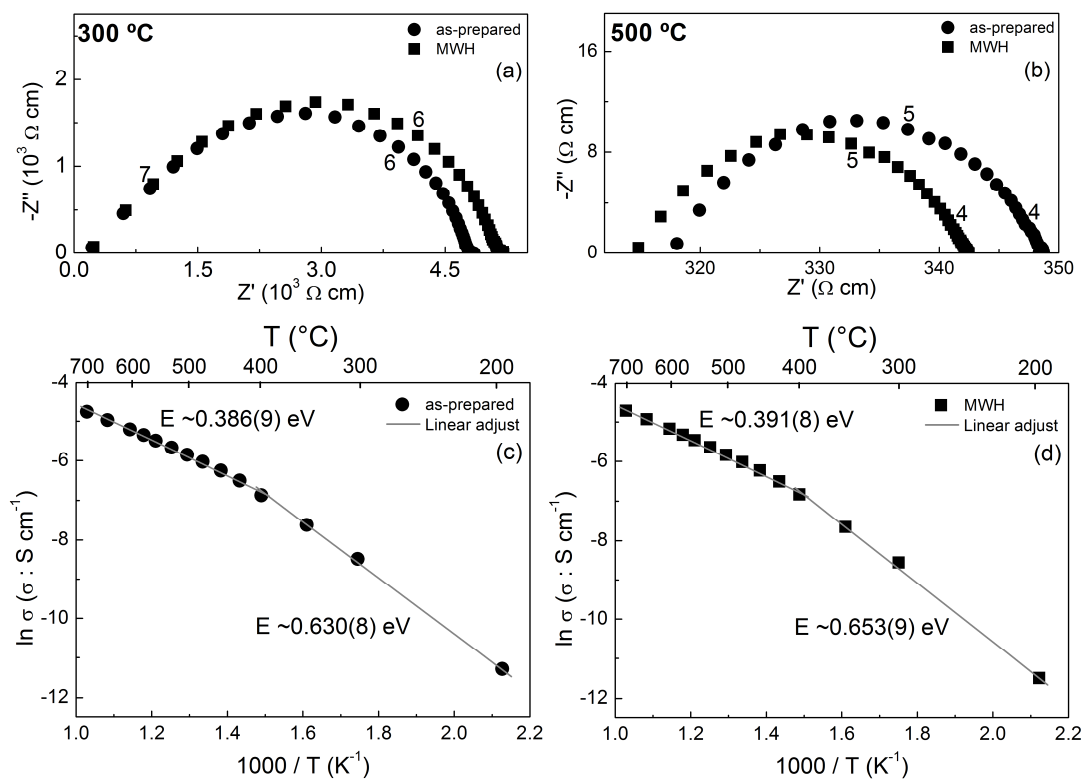


Figure 5 - Impedance diagrams measured at 300 °C (a) and 500 °C (b). Arrhenius plots for the total electrical conductivity for the as-prepared (c) and MWH (d) samples.

Summary

NiO/YSZ/CeO₂ (60/20/20 wt.%) composites were successfully synthesized by a coprecipitation-impregnation technique. Thermal analyses and X-ray diffraction indicate that microwave hydrothermal treatment promotes the crystallization of β -Ni(OH)₂ and CeO₂ while sintering resulted in the formation of the YSZ:CeO₂ solid solution. The microwave treated samples showed slightly higher densification as inferred from dilatometry analysis, but no significant differences were observed on the microstructure of sintered samples. Nonetheless, impedance spectroscopy analysis revealed that samples produced with microwave treatment have slightly higher activation energy and conductivity at temperatures > 450 °C.

References

- [1] N.Q. Minh, Ceramic fuel cells, *J. Am. Ceram. Soc.* 76 (1993) 563-588.
- [2] P.I. Cowin, C.T.G. Petit, R. Lan, J.T.S. Irvine, S. Tao, Recent Progress in the Development of Anode Materials for Solid Oxide Fuel Cells, *Adv. Energy Mater.* 1 (2011) 314-322.
- [3] D.S. Mclachlan, M. Blaszkiewicz, R.E. Newnham, Electrical-resistivity of composites, *J. Am. Ceram.Soc.* 73 (1990), 2187-2203.
- [4] D. Segal, Chemical synthesis of ceramic materials, *J. Mater. Chem.* 7 (1997) 1297-1305.
- [5] E. Vincenzo, D.Z. de Florio, F.C. Fonseca, E.N.S. Muccillo, R. Muccillo, E. Traversa, Electrical properties of YSZ/NiO composites prepared by a liquid mixture technique, *J. Eur. Ceram. Soc.* 25 (2005) 2637-2641.
- [6] A. Ringuedé, D. Bronine, J.R. Frade, Assessment of Ni/YSZ anodes prepared by combustion synthesis, *Solid State Ionics* 146 (2002) 219-224.
- [7] P.G. Keech, D.E. Trifan, V.I. Birss, Synthesis and performance of sol-gel prepared Ni-YSZ cermet SOFC anodes, *J. Electrochem. Soc.* 152 (2005) A645-A651.
- [8] M. Marinsek, K. Zupan, J. Macek, Preparation of Ni-YSZ composite materials for solid oxide fuel cell anodes by gel-precipitation method, *J. Power Sources* 86 (2000) 383-389.
- [9] G.A. Tompsett, W.C. Conner, K.S. Yngvesson, Microwave synthesis of nanoporous materials, *Chem Phys Chem* 7 (2006), 296-319.
- [10] S. Shi, J.-Y.Hwang, Microwave-assisted wet chemical synthesis: advantages, significance, and steps to industrialization, *J. Min Mater. Charact. Eng.* 2 (2003) 101-110.
- [11] E.T. Thostenson, T.-W. Chow, Microwave processing: fundamentals and applications, *Composites: Part A* 30 (1999) 1055-1071.
- [12] D.E. Clark, W.H. Sutton, Microwave processing of materials, *Annu. Rev. Mater. Sci.* 26 (1996) 299-331.
- [13] T. Subbaiah, R. Mohapatra, S. Mallick, K.G. Misra, P. Singh P, R.P. Das, Characterization of nickel hydroxide precipitated from solutions containing Ni²⁺ complexing agents, *Hydrometallurgy* 68 (2003) 151-157.
- [14] W.K. Yoshito, V. Ussui, D.R.R. Lazar, J.O.A. Paschoal, Synthesis and characterization of NiO-8YSZ powders by coprecipitation route, *Mater. Sci. Forum* 498-499 (2005) 612-617.
- [15] B. Djuricic, S. Pickering, Nanostructured cerium oxide: Preparation and properties of weakly agglomerated powders, *J. Eur. Ceram. Soc.* 19 (1999) 1925-1934.
- [16] P.-L. Chen, I.-W.Chen, Reactive cerium (IV) oxide powders by the homogeneous precipitation method, *J. Am. Ceram. Soc.* 76 (1993) 1577-1583.
- [17] P. Jeevanandam, Y. Koltypin, A. Gedanken, Synthesis of nanosized α -nickel hydroxide by a sonochemical method, *Nano Letters* 1 (2001) 263-266.
- [18] Q. Song, Z. Tang, H. Guo, S.L.I Chan, Structural characteristics of nickel hydroxide synthesized by a chemical precipitation route under different pH values, *J. Power Sources* 112 (2002) 428-434.
- [19] C. Wang, Y. Wang, W. Huang, B. Zou, Z.S. Khan, Y.Zhao, J. Yang, X. Cao, Influence of CeO₂ addition on crystal growth behavior of CeO₂-Y₂O₃-ZrO₂ solid solution, *Ceram. Int.* 38 (2012) 2087-2094.
- [20] F.C. Fonseca, D.Z. de Florio, V. Esposito, E. Traversa, E.N.S. Muccillo, R. Muccillo, Mixed ionic-electronic YSZ/Ni composite for SOFC anodes with high electrical conductivity, *J. Electrochem. Soc.* 153 (2006) A345-A360.

Electroceramics VI

10.4028/www.scientific.net/AMR.975

Effects of Microwave Processing on the Properties of Nickel Oxide/Zirconia/Ceria Composites

10.4028/www.scientific.net/AMR.975.154

DOI References

- [1] N.Q. Minh, Ceramic fuel cells, *J. Am. Ceram. Soc.* 76 (1993) 563-588.
<http://dx.doi.org/10.1111/j.1151-2916.1993.tb03645.x>
- [2] P.I. Cowin, C.T.G. Petit, R. Lan, J.T.S. Irvine, S. Tao, Recent Progress in the Development of Anode Materials for Solid Oxide Fuel Cells, *Adv. Energy Mater.* 1 (2011) 314-322.
<http://dx.doi.org/10.1002/aenm.201100108>
- [3] D.S. Mclachlan, M. Blaszkiewicz, R.E. Newnham, Electrical-resistivity of composites, *J. Am. Ceram. Soc.* 73 (1990), 2187-2203.
<http://dx.doi.org/10.1111/j.1151-2916.1990.tb07576.x>
- [5] E. Vincenzo, D.Z. de Florio, F.C. Fonseca, E.N.S. Muccillo, R. Muccillo, E. Traversa, Electrical properties of YSZ/NiO composites prepared by a liquid mixture technique, *J. Eur. Ceram. Soc.* 25 (2005) 2637-2641.
<http://dx.doi.org/10.1016/j.jeurceramsoc.2005.03.116>
- [6] A. Ringuedé, D. Bronine, J.R. Frade, Assessment of Ni/YSZ anodes prepared by combustion synthesis, *Solid State Ionics* 146 (2002) 219-224.
[http://dx.doi.org/10.1016/S0167-2738\(01\)00996-1](http://dx.doi.org/10.1016/S0167-2738(01)00996-1)
- [8] M. Marinsek, K. Zupan, J. Macek, Preparation of Ni-YSZ composite materials for solid oxide fuel cell anodes by gel-precipitation method, *J. Power Sources* 86 (2000) 383-389.
[http://dx.doi.org/10.1016/S0378-7753\(99\)00425-5](http://dx.doi.org/10.1016/S0378-7753(99)00425-5)
- [9] G.A. Tompsett, W.C. Conner, K.S. Yngvesson, Microwave synthesis of nanoporous materials, *Chem Phys Chem* 7 (2006), 296-319.
<http://dx.doi.org/10.1002/cphc.200500449>
- [12] D.E. Clark, W.H. Sutton, Microwave processing of materials, *Annu. Rev. Mater. Sci.* 26 (1996) 299-331.
<http://dx.doi.org/10.1146/annurev.ms.26.080196.001503>
- [13] T. Subbaiah, R. Mohapatra, S. Mallick, K.G. Misra, P. Singh P, R.P. Das, Characterization of nickel hydroxide precipitated from solutions containing Ni²⁺ complexing agents, *Hydrometallurgy* 68 (2003) 151-157.
[http://dx.doi.org/10.1016/S0304-386X\(02\)00203-7](http://dx.doi.org/10.1016/S0304-386X(02)00203-7)
- [14] W.K. Yoshito, V. Ussui, D.R.R. Lazar, J.O.A. Paschoal, Synthesis and characterization of NiO-8YSZ powders by coprecipitation route, *Mater. Sci. Forum* 498-499 (2005) 612-617.
<http://dx.doi.org/10.4028/www.scientific.net/MSF.498-499.612>
- [16] P. -L. Chen, I. -W. Chen, Reactive cerium (IV) oxide powders by the homogeneous precipitation method, *J. Am. Ceram. Soc.* 76 (1993) 1577-1583.
<http://dx.doi.org/10.1111/j.1151-2916.1993.tb03942.x>
- [17] P. Jeevanandam, Y. Koltypin, A. Gedanken, Synthesis of nanosized α -nickel hydroxide by a sonochemical method, *Nano Letters* 1 (2001) 263-266.
<http://dx.doi.org/10.1021/nl010003p>

[18] Q. Song, Z. Tang, H. Guo, S.L. I Chan, Structural characteristics of nickel hydroxide synthesized by a chemical precipitation route under different pH values, *J. Power Sources* 112 (2002) 428-434.

[http://dx.doi.org/10.1016/S0378-7753\(02\)00396-8](http://dx.doi.org/10.1016/S0378-7753(02)00396-8)

[19] C. Wang, Y. Wang, W. Huang, B. Zou, Z.S. Khan, Y. Zhao, J. Yang, X. Cao, Influence of CeO₂ addition on crystal growth behavior of CeO₂-Y₂O₃-ZrO₂ solid solution, *Ceram. Int.* 38 (2012) 2087-(2094).

<http://dx.doi.org/10.1016/j.ceramint.2011.10.046>